Clays and Clay Minerals, Vol. 52, No. 4, 495–509, 2004.

MINERALOGICAL AND CHEMICAL CHARACTERIZATION OF SEPIOLITE OCCURRENCES AT KARAPINAR (KONYA BASIN, TURKEY)

N. KARAKAYA[1], M. ÇELIK KARAKAYA[1], A. TEMEL[2], Ş. KÜPELI[1] AND C. TUNOĞLU[2]

[1] Selçuk Üniversitesi, Müh-Mim. Fakültesi, Jeoloji Mühendisligi Bölümü, 42031 Konya, Turkey
[2] Hacettepe Üniversitesi, Müh. Fakültesi, Jeoloji Mühendisligi Bölümü, 06535 Ankara, Turkey

Abstract—The Konya region in central Anatolia is covered by Pliocene–Late Pleistocene sediments and volcanites related to the sediments NNW of Karapınar, Turkey. In the area, the Upper Miocene–Quaternary Üzecek Dağı and Karacadağ volcanites are generally of the same age and formed from magmas of similar composition. The Karapınar formation is brown to whitish-beige, partly fossiliferous and consists of limestone, marl, claystone and, locally, sandy layers. Silica-rich lenses, nodules and layers are observed in the upper strata which locally contain sepiolite-rich layers. The mineralogical composition of sepiolite samples taken from the area was determined by powder X-ray diffractometry, while the abundance of major-element oxides was measured by X-ray fluorescence spectrometry. The crystallographic and morphological properties of samples were determined by means of scanning electron microscopy and energy dispersive spectroscopy. Samples were taken from three sections and from random locations. Mineral assemblages in the same stratigraphic position are generally similar in the three sections, while the thickness of the individual beds varies between the sections. Dolomite and calcite are the main carbonate minerals in the sections. Sepiolite occurs primarily with dolomite and, locally, dolomite and calcite, and less commonly with just calcite. Generally, quartz, feldspar and mica are found, especially in the upper parts of the sections where tuff is abundant. CaO and MgO dominate the major-element oxides. The CaO content is between 1 and 30% while MgO is 3−21%. Al_2O_3 and SiO_2 are generally higher in the sepiolitic and tuffitic layers. Al_2O_3 is <3% and SiO_2 is between 15−18% in the sepiolitic layers. The average structural formula of sepiolite was calculated as: $(Mg_{7.00}Al_{0.44}Fe_{0.18})(Si_{11.71}Al_{0.29})O_{30}(OH)_4(OH_2)_4Ca_{0.13}K_{0.09}Na_{0.01}$. Sepiolite occurs as fibers and dolomite as subhedral or euhedral crystals. It is considered that sepiolite was formed either by conversion of dolomite or by direct precipitation from solution under alkaline and saline conditions in the Karapınar paleolake. The paleolake was saturated with respect to Mg, Ca and Si derived from groundwater that percolated along fracture systems.

Key Words—Dolomite, Karapınar, Konya, Protodolomite, Sepiolite, Turkey.

INTRODUCTION

The Konya paleolake sediments contain abundant evidence of chemical precipitation. The sediments contain various components of evaporitic sequences usually described from continental environments (Collinson, 1978), including freshwater organisms, alkaline earth carbonates, sulfates (Ca, Na), halite and sepiolitic clays. Sepiolite and palygorskite are fibrous clay minerals commonly associated with phosphatic sediments, salt deposits, sulfates, carbonates, zeolites and siliceous rocks (Millot, 1970; Velde, 1985; Jones and Galán, 1988). Sepiolite beds have also been reported from playa-lake deposits in Nevada and California (Post, 1978; Hewett, 1956), Saudi Arabia (Shadfan *et al*., 1985) and Spain (Galán and Ferrero, 1982; Mayayo *et al*., 1998). Turkey has abundant large sedimentary deposits of sepiolite, some of which have been studied, particularly with regard to their mineralogical characterization and environments of formation (Ece and Çoban, 1994; Ece, 1998; Kadir *et al*., 2002; Yeniyol, 1995). There are however, no reports of sepiolite occurrences in the study area.

* E-mail address of corresponding author:
mzzclk@hotmail.com
DOI: 10.1346/CCMN.2004.0520410

Preliminary studies on the Karapınar sepiolite occurrences were reported by Karakaya *et al*. (2001) (M.Ç. Karakaya, N. Karakaya, A. Temel, Ş. Küpeli and Ü. Demiray, unpublished DPT/SÜAF report, 2001). The Neogene lacustrine basin east of Konya contains a sedimentary sequence in which sepiolite and palygorskite are found associated mainly with calcite and dolomite, although their abundance varies significantly both vertically and laterally. The mineral assemblages and occurrence of the Karapınar sepiolite are quite different from the Yunak (Yeniyol, 1995) and Eskisehir (Ece and Çoban, 1994; Ece, 1998) sepiolites, but similar to the Pinarbasi sepiolite (north of Konya) (M.Ç. Karakaya, N. Karakaya, A. Temel, Ş. Küpeli and Ü. Demiray, unpublished DPT/SÜAF report, 2001; Kadir *et al*., 2002). The sepiolite occurs in both medium- and thick-bedded, brown or white sedimentary layers. The purpose of this study is to determine the textural, chemical and mineralogical characteristics of the sepiolite, to analyze the depositional paleoenvironments of the Late Miocene to Pleistocene sediments of the Konya lacustrine basin, and to compare these deposits with the other Neogene carbonate and sepiolite-palygorskite occurrences in Turkey in order to broadly evaluate their genetic relationships.

MATERIALS AND METHODS

In this study, 120 samples were collected from three sections and also from spot locations (Figure 1). The mineralogical characteristics of the samples were determined by X-ray diffraction (XRD) and scanning electron microscopy (SEM)-energy dispersive spectroscopy (EDS) techniques. Chemical analyses of the samples were done by wavelength dispersive X-ray fluorescence (XRF) spectrometry. The mineralogical composition of the bulk-rock and clay-size fractions (<2 μm) were determined using a Philips PW 1140 X-ray powder diffractometer with a graphite monochromator and Ni-filtered CuKα radiation. Powder diffraction data were corrected using NaCl as an internal standard. Powders were scanned at 1º2θ/min from 2 to 70º2θ. The proportions of the minerals were calculated from powder XRD patterns using an internal standard method (Gündoğdu, 1982). The relative accuracy of this method is within ±15%. All powdered samples were prepared using an automatic agate mortar and pestle system. Glass slides with shallow cavities were filled with powders for randomly oriented specimens. Marl and carbonate-rich samples were decomposed in a warm, dilute HCl solution to obtain the clay fractions (Jackson, 1975). The <2 μm clay fractions of the samples were washed three times with deionized water by centrifuging the slurry in order to get rid of excess cations which may cause flocculation. The <2 μm clay fractions were obtained on the basis of Stokes' law, and excess water was removed by centrifuging. Smear glass samples were prepared from the remaining clay fractions (Gibbs, 1965, 1968). Clay minerals were identified from three XRD patterns of the clay-sized fractions, air dried at 25ºC, ethylene glycolated, and heated at 490ºC for 4 h.

Differential thermal analysis (DTA)-thermogravimetric (TG) analysis was carried out using a Rigaku 2.22E2 instrument by heating ~20 mg of the specimen in the range 20−900ºC (at a heating rate of 10ºC/min) using α-Al_2O_3 as a reference material. The SEM studies were carried out using a JSM 6400 model SEM, equipped with EDS using an accelerating voltage of 25 kV. Spot chemical analyses of sepiolite, palygorskite and carbonate minerals were carried out using wavelength dispersive spectrometry (WDS). A JSM-6400 scanning electron microscope was used at 15 kV accelerating voltage, a beam current of 15 nA, a beam diameter of 5 μm and with a ZAF correction scheme (Albee and Ray, 1970). Analyses for major elements of the clay samples were performed using a Philips PW 1480 model X-ray fluorescence spectrometer. The weight percentages of major elements were determined on fused disks (prepared with 0.75 g of rock powder and 4.5 g of lithium tetraborate) (Brown *et al*., 1973; Temel *et al*., 1998). The spectrometers were calibrated using international standards (Flanagan, 1976; Govindaraju, 1989).

Loss on ignition (LOI) was calculated from weight loss after heating 2 g of sample at 1000ºC for 2 h. Chemical analyses of clay-sized fractions were used to calculate the structural formulae of clay minerals, based on 32 oxygen atoms for sepiolite (Bain and Smith, 1987; Weaver, 1989). The following assumptions for sepiolite were used: (1) the tetrahedral sites are filled with Si and Al to sum to 12; (2) Mg is octahedral and all Fe is ferric; (3) the remainder of Al is octahedral; and (4) Ca, K and Na are exchangeable interlayer cations. The $MgCO_3$ content of calcite and dolomite was obtained by measuring the d_{104} values (Goldsmith *et al*., 1961). The precise position of the d_{104} peak was obtained by referring to halite, which has a major peak close to the main calcite peak, as an internal standard.

GEOLOGICAL SETTING

The study area is located in the Tuz Gölü basin, a remnant of the Konya paleolake, ~90 km east of Konya (Figure 1). The basin is ~200 km long and 100 km wide, and seven different periods of evaporative formation, from the Late Cretaceous to the Pliocene, have been determined (M. Yaşar, E. Çelik, S. Kayakıran, M.C. Erkan, M. Aygün, F. Ayok, H. Baş, T. Bilgiç, A. Uygun, 1982, unpublished MTA report). During the Maastrichtian to Eocene, the basin was of inner shallow marine character, while in the Late Miocene it was a closed lake. The authors indicated that concentrations of some ions, *e.g.* Mg^{2+}, Na^{+}, K^{+}, HCO_3^{-}, Cl^{-} and SO_4^{2-}, are quite high, and Ca^{2+} is relatively high in groundwaters. The concentrations of these ions were found to be 3000−4000, 35,000−66,000, 600−1600, 400−1100, 46,000−94,000, 16,000−27,000 ppm, respectively, and there is 400−800 ppm Ca in groundwater (at 3.5−30 m depth), in places ~30−40 km north of Karapınar.

The Tuz Gölü basin can be divided into small lacustrine basins, *e.g.* the Karapınar, Cihanbeyli, Beysehir, Aksaray basins, on the basis of depressions or small fault systems (Figure 1). From the Miocene to the Recent, the basins were partially or completely dried and different types of evaporative minerals, *e.g.* salts (halite, sylvite), gypsum, carbonates, borates and sulfates (Na), were deposited in the basins.

Pre-Neocene ophiolitic mélange and recrystallized limestone units comprise the basement in the study area (A.M. Özgüner, M. Büyüktemiz, A. Murat and O. Gökmenoğlu, 1993, unpublished MTA report). The basement units are overlain by a Pliocene–Late Pleistocene sepiolite-bearing lacustrine sedimentary succession. The sedimentary succession consists of clayey limestone, calcareous clay, dolomite, different types of salts, gypsum-bearing lacustrine clayey material and volcanites (tuffs). During the Late Miocene–Pliocene, volcanism produced mainly tuff and lesser volcanic breccia and agglomerate, and also lava flows of andesitic, basalt-andesitic and basaltic compositions in

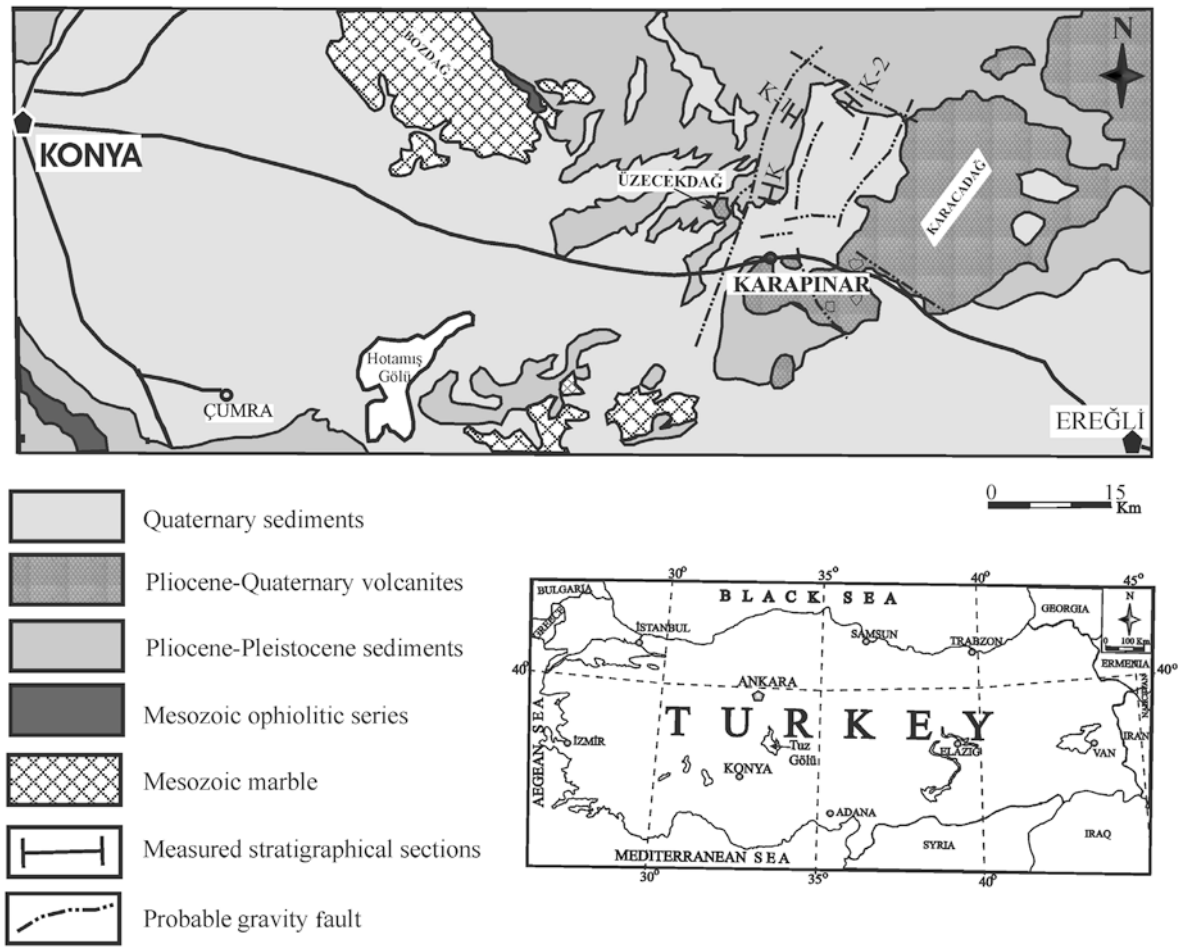

Figure 1. Geological map of the study area.

different episodes. The volcanic rocks are generally purple and porphyritic, and are composed of amphibole, biotite and plagioclase (Aydar, 1989). Ash cones, maars and emanations formed in the Late Pleistocene–Quaternary. The volcanic activity produced olivine-basalts, basaltic andesites and tuffs. These volcanic rocks have hypohyaline porphyritic texture and consist of plagioclase, olivine, clinopyroxene and hornblende (Aydar, 1989; Ercan *et al*., 1992; Olanca, 1999). The thickness of the tuff layers ranges from 5 cm to 1 m and these layers alternate with carbonate and sepiolitic carbonate layers in all sequences. The tuff layers generally contain broken or embayed biotite crystals.

In the study area, the precipitation of lacustrine carbonates occurred when volcanic activity was waning or had ceased, and the carbonates grade into volcanites horizontally and vertically. Three types of sepiolite-carbonate beds are recognized in the different parts of the basin: (1) organic matter-rich brown sepiolite (with gastropods, ostracods and plant fossils); (2) organic matter-poor sepiolite, which contains ~50% dolomite; and (3) white–cream-colored carbonate layers, which are generally composed of dolomite and/or calcite and lesser amounts of sepiolite (~5–20%), or pure carbonate minerals.

Carbonate-sepiolite occurrences occur throughout the Tuz Gölü basin, and in some parts of the basin, one or two carbonate minerals are dominant. Dolomite is the main carbonate mineral in and around Tuz Gölü itself. Dark brown layers (10–50 cm) are thinner than the other layers and have been observed only in the deeper parts of the basin. Brown, organic matter-rich sepiolite beds are overlain by light-brown, discontinuous dolomitic layers. White to cream-colored carbonate layers have generally been observed in the upper parts of the sequences and contain opal lenses (5–120 cm) or silica nodules of various shapes. The outer parts of the silica nodules and opal lenses have thin (0.5–1 cm) coatings of carbonate minerals, mainly dolomite. The silica-rich layers are 10–80 cm thick. All types of the carbonate-sepiolite occurrences were sampled in the three sections and from spot locations (Figure 2). An increase in silica precipitation, occurring as irregular and discontinuous layers, has been observed locally in the upper parts of the sequence

https://doi.org/10.1346/CCMN.2004.0520410 Published online by Cambridge University Press

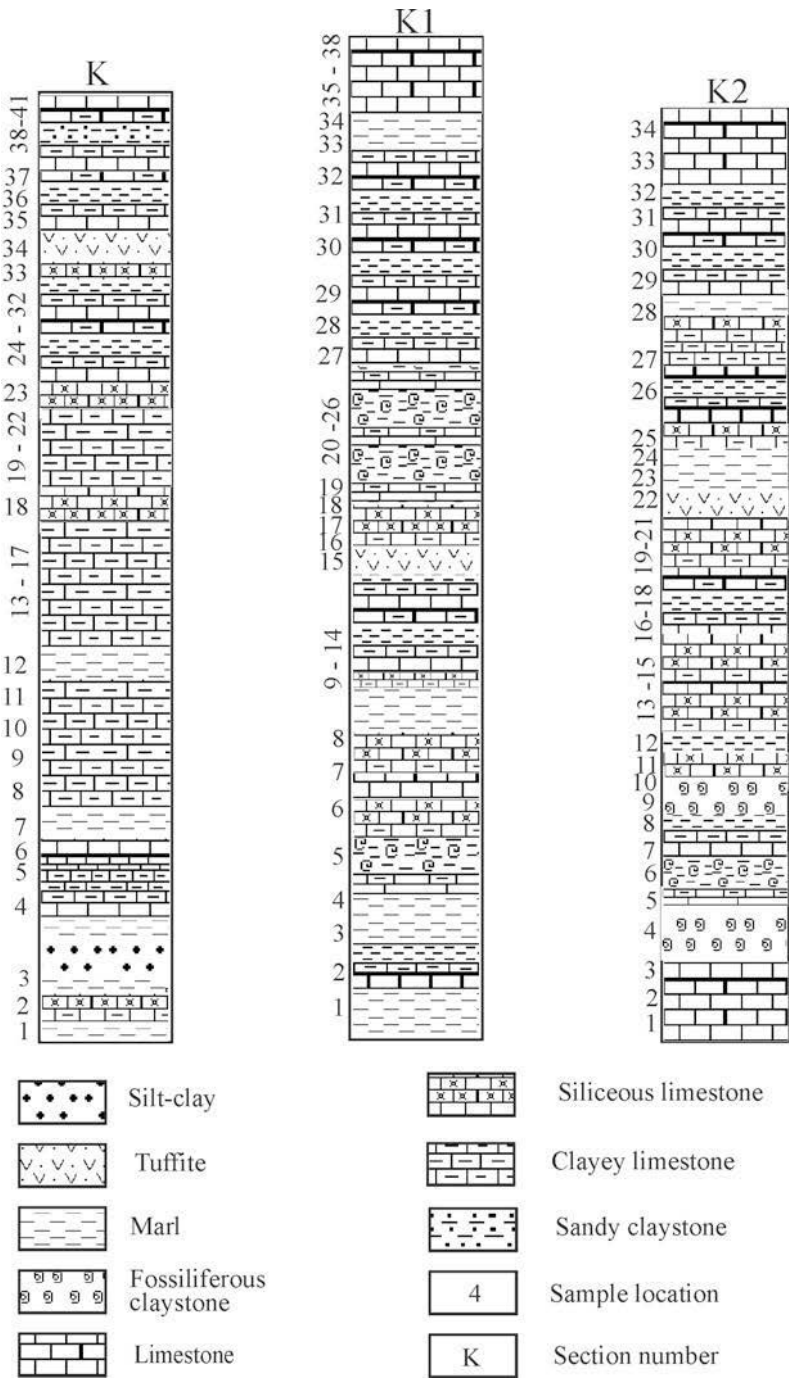

Figure 2. Distribution of the principal lithologies in the study area (see Figure 1 for section locations, and Table 1 for mineralogical composition, types and relative abundances of minerals in the samples).

or, rarely, above the sepiolitic layers. The precipitation of silica-rich layers suggests that siliceous gel precipitated from supersaturated solution during carbonate sedimentation and/or after sepiolite precipitation (Figure 2) caused by changes in the chemical character of the lake.

RESULTS

The lacustrine carbonates are generally micritic and consist mainly of dolomite and calcite in varying proportions, not only in the Karapınar basin but also in the north of the basin around Tuz Gölü (Figure 1). Huntite, ulexite and gypsum are widespread in the

https://doi.org/10.1346/CCMN.2004.0520410 Published online by Cambridge University Press

Karapınar basin. Also, deposits of halite, sylvite and sodium sulfate minerals (thenardite, glauberite, *etc*.) were found during drilling (A.M. Özgüner, M. Büyüktemiz, A. Murat, and O. Gökmenoğlu, 1993, unpublished MTA report). Dolomite is generally present in all layers and is also the main carbonate mineral, but calcite occurs as a main carbonate mineral in a few layers, and is especially abundant in the upper parts of the sections I and II (Figure 2, Table 1). Sepiolite is generally observed with dolomite, locally with dolomite and calcite, and in some cases with calcite. Lesser amounts of feldspar, biotite, hornblende, quartz, palygorskite and muscovite occur in some layers. These mineral assemblages are typically not uniform in the vertical and horizontal directions, and different parageneses characterize the sections.

Based on XRD studies, a clear difference has been recognized in the mineral assemblages of the sepiolites, between the white (KI-5, 33, 36), the cream-colored (K-5, 11) and the brown organic matter-rich (KII-4, 9) material (Figure 3, Table 1), but the crystallinity of the organic-matter rich sepiolites is better than that of the white and cream-colored sepiolites. Identification was performed according to JCPDS (1993). Some patterns indicate that sepiolite is poorly ordered so that not all diffraction lines for sepiolite could be identified in all powder XRD patterns. Typical XRD patterns of the sepiolite are given in Figure 3. The most intense and diagnostic reflections are from the (110) planes, yielding a strong maximum at 12.28 Å in sepiolite and at 10.30 Å in palygorskite. Other moderate-intensity reflections for sepiolite are at 4.5 Å (060), 4.3 Å (131), 3.75 Å (260) and 3.20 Å (331), and for palygorskite at 6.36 Å (200), 4.47 Å (040), 4.26 Å (121) and 3.68 Å (221). The sharpness and intensities of the diffraction lines are comparable to those of the Eskişehir (Ece and Çoban, 1994) and Hekimhan sepiolites (Yalçın and Bozkaya, 1995) suggesting moderate–low crystallinity of the material. The 110 peaks of the oriented sepiolite samples collapsed from 12.28 to 10.4 and 8.2 Å after heat treatment. Following glycolation, there was no swelling in palygorskite, whereas a slight expansion from 12.28 to 12.64 Å was observed, accompanied by contraction of the 130 spacing from 4.53 to 4.48 Å (Figure 4). Similar properties were also observed in the Eskişehir (Ece and Çoban, 1994), Hekimhan (Yalçın and Bozkaya, 1995) and Yunak sepiolites (Yeniyol, 1986). A broad, weak reflection related to the sepiolite peak in the 10−12 Å range during normal diffraction, with an average value at 11 Å, was observed in some samples; this reflection was attributed to palygorskite. Opal-CT peaks at 4.33, 4.11 and 2.51 Å were observed in XRD analysis of silica-rich bands and nodules.

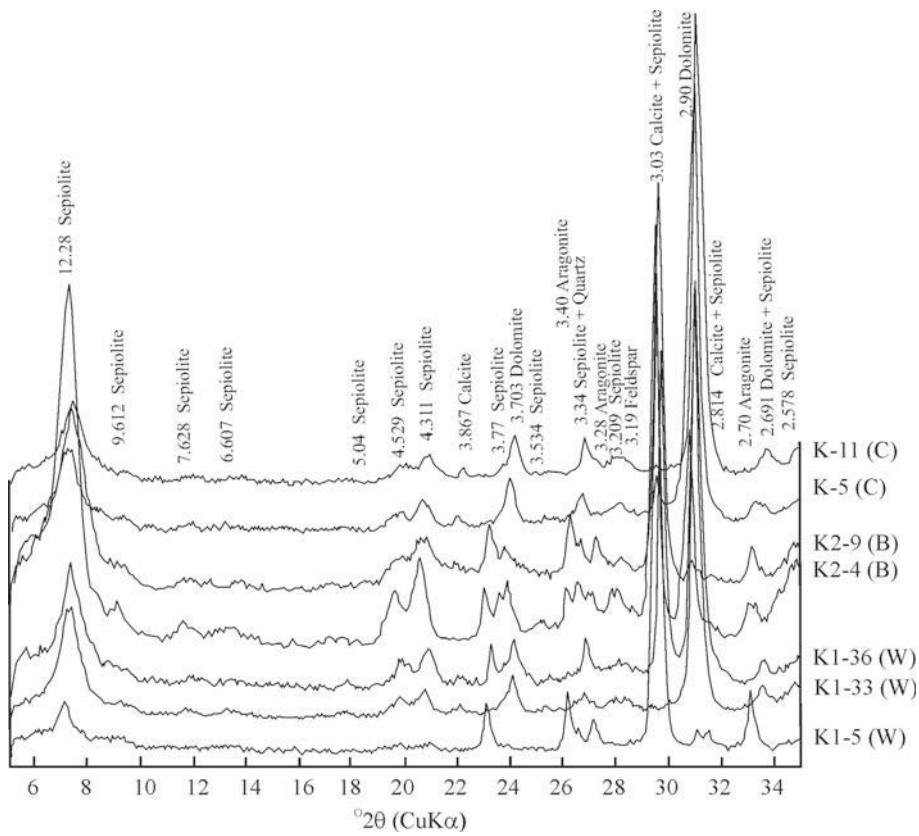

Figure 3. Whole-rock XRD patterns of some samples from the sampled sections. Non-oriented samples; peak spacings in Å.

https://doi.org/10.1346/CCMN.2004.0520410 Published online by Cambridge University Press

Table 1. Mineralogical composition, types and variation of stratigraphic sections samples and random samples.

S.N.	S.C.	Do	Ca	Se	Qu	Pa	Fe	Ar	Amp	Mi	S.N.	S.C.	Do	Ca	Se	Qu	Pa	Fe	Ar	Amp	Mi
K-1	W	+++	+++++	++							KI-15	W				++		+++++			++
K-2	W	+++++		++++		++					KI-16	W	+++++		+						
K-3	W	++	+++++	++							KI-17	W	+++++		++						
K-4	C	+++++	++	++++			++				KI-18	W	+++++		++						
K-5	C	+++++	++	++++			++				KI-19	C	+++++		++						
K-6	C	+++++		+++							KI-20	C	+++++	++++	+++						
K-7	C	+++	+++++	++	++						KI-21	W		+++++			++				
K-81	C	+++++		+++							KI-22	W	+++	+++++	++						
K-82	C	+++++		+++							KI-23	C	+++	+++++	++++		++			++	
K-83	C	+++++		++							KI-24	W	+++++		+			++			
K-9	C	+++++		++++							KI-25	W	+++++		+						
K-10	C	+++++		++++							KI-26	W	+++++		++						
K-11	C	+++++		++++	++						KI-27	W	+++++		++						
K-12	C	+++++		+++							KI-28	W	+++++		++						
K-13	W	+++++		+++							KI-29	C	+++++		++++						
K-14	W	+++	+++++								KI-30	W	+++++		++						
K-15	C	+++++		++++							KI-31	W	+++++		++						
K-16	W	+++++		+++							KI-32	W	+++++		++						
K-17	W	+++++		+++							KI-33	W	++++		++++						
K-18	C	+++++		++++					++		KI-34	C	++++	+++	++++					++	
K-19	C	+++++		+++							KI-35	C	++++	+++	++++	++					
K-20	W	+++++		+							KI-36	C	++++	++++	++++					+	
K-21	W	+++++		+							KI-37	W	++++	++++	+++		++	+			
K-22	W	+++++		+++							KI-38	W	+++	+++++	+						
K-23	W	+++++		+++							KII-1	W	+++++		+						
K-24	W	+++++		+							KII-2	W	+++++		+						
K-30	C	+++++		++++							KII-3	W	+++++		+						
K-31	C	+++++		++							KII-4	B	++++	++++	++++			++	++		
K-32	W	++	+++++		++	+	+				KII-5	W	+++++		+						

Table 1 (*contd.*)

S.N.	S.C.	Do	Ca	Se	Qu	Pa	Fe	Ar	Amp	Mi	S.N.	S.C.	Do	Ca	Se	Qu	Pa	Fe	Ar	Amp	Mi
K-33	C	++	+++++		++	+					KII-6	B	+++	+++++	++++		++			++	
K-34	C		++		++++		+++		+++		++	KII-7	W	+++++		++					
K-35	C	+++++		++							KII-8	B	+++++		++						
K-36	C	+++++		++							KII-9	B	+	+++++	+++++			+++		+++	++	
K-37	C	+++++		+							KII-10	C	+++++	+++	+++						
K-38	W	+++++	++		++	++					KII-11	W	+++++		+++						
K-39	C	+++++			++	++	++				KII-12	W	+++++		+++						
K-40	C	+	+++++	+	++	++	++				+ KII-13	W	+++++		+++						
K-41	W	++	+++++		++						KII-14	W	++++	+++++	+++					++++	
K-42	W	++	+++++		++	++					KII-15	C	+++++		+++						
K-43	W	++++	++++	++	++	+++			++		KII-16	W	+++++		++++						
K-44	W	++++		++	++	++					KII-17	W	+++++		+++						
K-45	W	++++	++++	+		+					KII-18	W	+++++		+++						
K-46	C	+++++		++++			+				KII-19	W	+++++	+	++++						
K-47	W	+++++	+++	+							KII-20	C	+++++	+++	+++						
K-48	C	++++	+++++		+						KII-21	W		+++++	+						
K-49	W	++++	+++++		+						KII-22	C	+++++	+	+++						
K-50	W	+++++		+							KII-23	C	+++++		++						
KI-1	C	+++++	+++	+		++					KII-24	C	+++++		++			+			
KI-2	W	+++++		++							KII-25	W	+++++		++++						
KI-3	W	+++++		++							KII-26	W	+++++		++++	++		++			
KI-4	W		+++++	+	++						KII-27	W	+++++		++						
KI-5	W		+++++	+				+++			KII-28	W	+++++		++						
KI-6	W	+++++	++++	++		+					KII-29	W	+++++		++++						
KI-7	W	++++	++++	++							KII-30	W	+++++		++						
KI-8	W	+	+++++						++++		KII-31	C	+++++		++++			++			
KI-9	W	+	+++++	+							KII-32	C	+++++		+++						
KI-11	W	++++	++++	+		+					KII-33	C		+++++	++						
KI-13	C	+++++		+++							KII-34	C		+++++	++						
KI-14	C	+++++		++++																	

S.N.: Sample name; S.C.: Sample color; C: cream, W: white, B: brown sepiolite; Do: dolomite, Ca: calcite, Se: sepiolite, Pa: palygorskite, Qu: quartz, Fe: feldspar, Ar: aragonite, Amp: amorph silica (Opal, Opal-CT), Mi: Mica; +: relative abundance of mineral.

Table 2. Major element oxide composition of whole rock-samples (%) and some statistical parameters of each sequence.

Oxide		SiO_2	Al_2O_3	Fe_2O_3	CaO	MgO	K_2O	Na_2O	TiO_2	Mn_2O_3	P_2O_5	Cr_2O_3	LOI	Total
K-4	C	14.49	0.96	0.35	24.87	19.69	0.07	0.09	0.05	0.01	–	0.01	38.15	98.74
K-5	C	15.97	1.33	0.52	25.86	17.78	0.15	0.11	0.06	0.01	–	0.01	36.99	98.76
K-81	C	8.64	0.74	0.29	26.81	20.72	0.08	0.10	0.04	0.01	–	0.01	41.80	99.22
K-82	C	15.52	1.10	0.46	23.78	20.28	0.12	0.09	0.06	0.01	–	0.01	37.68	99.11
K-9	C	14.37	1.22	0.52	24.12	20.20	0.16	0.08	0.07	0.01	–	0.01	38.24	99.01
K-10	C	7.82	0.61	0.21	25.98	21.03	0.06	0.10	0.03	0.01	–	0.01	42.45	98.32
K-11	C	20.56	2.49	0.85	20.68	19.08	0.41	0.15	0.12	0.02	0.01	0.01	34.41	98.79
K-12	C	14.70	2.00	0.90	23.78	19.41	0.30	0.10	0.10	0.02	0.01	0.01	38.02	99.35
K-13	W	8.72	1.21	0.50	25.00	19.56	0.15	0.09	0.07	0.01	0.01	0.01	40.42	95.74
K-15	C	16.69	1.23	0.44	21.93	21.12	0.16	0.16	0.06	0.01	0.01	0.01	36.87	98.70
K-16	W	11.81	0.85	0.26	24.61	21.13	0.10	0.14	0.04	0.01	–	0.01	40.21	99.16
K-18	C	19.37	0.11	0.01	23.72	18.69	–	0.06	–	–	–	0.01	37.37	99.31
K-19	C	13.06	1.08	0.41	24.65	20.06	0.10	0.13	0.05	0.01	–	0.01	39.04	98.61
K-23	W	14.27	1.81	0.63	24.98	18.03	0.20	0.18	0.10	0.01	–	0.01	38.18	98.39
K-30	C	14.56	0.75	0.28	23.86	21.34	0.06	0.07	0.04	0.01	–	0.01	38.16	99.11
K-31	C	8.37	0.83	0.35	26.49	20.63	0.09	0.08	0.04	0.01	–	0.01	41.76	98.65
K-34	C	57.20	14.95	7.62	1.15	4.71	2.52	0.16	0.76	0.03	0.01	0.03	7.61	96.76
K-40	C	34.19	8.98	4.14	21.98	3.37	1.60	0.15	0.45	0.08	0.08	0.02	22.09	97.52
K-43	W	21.00	5.59	2.36	27.68	8.62	1.04	0.11	0.24	0.07	–	0.01	31.63	98.38
K-44	W	21.28	5.56	2.38	26.98	9.17	1.01	0.09	0.24	0.06	0.02	0.01	32.12	98.93
K-46	C	16.11	1.52	0.67	24.36	18.83	0.16	0.08	0.08	0.02	–	0.01	37.49	99.34
Max		57.20	14.95	7.62	27.68	21.34	2.52	0.18	0.76	0.08	0.08	0.03	42.45	99.35
Min		7.82	0.11	0.01	1.15	3.37	0.06	0.06	–	0.01	0.01	0.01	7.61	95.74
Mean		18.24	2.84	1.27	23.08	17.08	0.47	0.11	0.14	0.02	0.02	0.01	35.26	98.52
SS		11.98	3.87	1.96	6.17	5.76	0.69	0.03	0.19	0.02	0.03	0.01	8.62	0.96
KI-3	W	8.19	0.59	0.43	27.31	19.66	0.09	–	0.04	0.01	0.01	–	42.51	98.85
KI-4	W	3.13	0.21	0.27	51.15	2.10	0.03	–	0.02	0.01	0.01	–	42.81	99.74
KI-6	W	7.71	0.47	0.18	32.45	16.16	0.04	0.08	0.03	0.01	–	0.01	41.94	99.08
KI-7	W	11.17	0.41	0.17	35.81	10.94	0.05	0.09	0.02	0.01	–	0.01	4-	98.65
KI-9	W	4.57	0.33	0.33	49.63	2.94	0.06	–	0.03	–	0.02	–	42.00	99.91
KI-11	W	11.34	0.99	0.53	27.61	18.33	0.14	–	0.05	0.01	0.01	–	40.45	99.26
KI-13	C	13.43	1.09	0.40	24.71	20.17	0.13	0.09	0.05	0.01	–	0.01	39.06	99.14
KI-14	C	15.42	1.04	0.40	24.57	18.88	0.13	0.22	0.05	0.01	–	0.01	37.97	98.70
KI-15	W	58.16	14.95	3.90	6.78	3.39	2.54	3.00	0.47	0.08	0.25	–	3.79	97.32
KI-19	C	13.36	0.98	0.39	24.29	19.53	0.12	0.18	0.05	0.01	0.01	39.01	97.92	
KI-21	W	10.71	0.24	0.13	47.46	0.68	0.02	–	0.01	0.03	–	–	38.70	98.08
KI-23	C	14.74	2.27	0.90	36.96	7.22	0.42	–	0.10	0.03	–	–	35.88	98.54
KI-25	W	2.54	0.21	0.05	30.09	18.82	–	–	0.01	–	–	–	46.25	97.99
KI-29	C	13.91	1.27	0.54	23.64	19.86	0.18	0.08	0.06	0.01	–	0.01	38.79	98.36
KI-33	W	15.81	0.47	0.22	23.77	20.80	0.05	0.07	0.02	0.01	–	0.01	37.79	99.00
KI-34	C	13.11	1.71	0.67	24.52	19.41	0.26	0.08	0.07	0.01	–	0.01	39.35	99.20
KI-35	C	15.74	1.75	0.76	28.59	14.99	0.25	0.09	0.09	0.02	–	0.01	36.60	98.89
KI-36	C	16.11	1.99	0.90	29.10	14.19	0.29	0.08	0.10	0.02	–	0.01	36.18	98.97
KI-37	W	9.55	0.73	0.28	34.23	14.06	0.07	0.04	0.03	0.01	–	0.01	40.13	99.14
Max		58.16	14.95	3.90	51.15	20.80	2.54	3.00	0.47	0.08	0.25	0.01	46.25	99.91
Min		2.54	0.21	0.05	6.78	0.68	0.02	0.04	0.01	–	–	–	3.79	97.32
Mean		13.62	1.67	0.60	30.67	13.80	0.27	0.34	0.07	0.02	0.05	0.01	37.85	98.78
SS		11.59	3.28	0.84	10.51	7.03	0.58	0.84	0.10	0.02	0.10	–	8.64	0.64

The DTA-TG analyses were performed on cream-colored and brown sepiolite obtained from clay fractions (samples K-5 and KII-9). A large, broad endothermic peak was observed at 97ºC and 106ºC, due to the loss of sorbed water (dehydration), and a second small endothermic peak occurs at 436 and 445ºC, related to OH release and decomposition. Exothermic reactions were seen as an intense peak at 824 and 831ºC. Weight losses accompanying endothermic reactions were ~9 and 12%, respectively, and 2% of exothermic reactions.

The results of chemical analyses are presented in Tables 2 and 3. According to statistical parameters (arithmetic mean, standard deviation, *etc.*), Al_2O_3, Fe_2O_3, K_2O and some SiO_2 values are lower in section KII than in sections K and KI, while CaO values are less in section K than in the other sections. Al, Na, K, Fe and Ti (expressed as oxides) are present only in very small amounts in all layers, except in the tuffitic layers (Table 2). SiO_2 and MgO values are higher in sepiolitic layers than in the carbonate layers. The variation of SiO_2

https://doi.org/10.1346/CCMN.2004.0520410 Published online by Cambridge University Press

Table 2 (*contd.*)

Oxide		SiO_2	AlO_3	Fe_2O_3	CaO	MgO	K_2O	Na_2O	TiO_2	Mn_2O_3	P_2O_5	Cr_2O_3	LOI	Total
KII-3	W	5.51	0.71	0.25	28.60	20.36	0.08	–	0.03	0.01	–	–	44.02	99.60
KII-4	B	15.74	1.75	0.76	28.59	14.99	0.25	0.09	0.09	0.02	–	0.01	36.60	98.89
KII-5	W	5.86	0.60	0.42	30.46	19.99	0.12	–	0.03	0.01	0.02	–	43.73	101.26
KII-6	B	17.52	2.01	0.66	33.84	9.01	0.30	0.08	0.09	0.01	0.01	0.01	35.10	98.65
KII-8	B	7.83	0.55	0.38	29.27	20.14	0.09	–	0.03	0.01	0.03	–	42.76	101.10
KII-9	B	31.46	0.80	0.35	25.82	13.24	0.11	0.06	0.04	0.01	–	0.01	26.91	98.79
KII-11	W	6.46	0.43	0.35	30.47	20.12	0.08	–	0.03	0.01	0.02	–	43.34	101.31
KII-14	W	45.90	0.31	0.29	23.83	5.71	0.06	–	0.02	0.01	0.01	–	24.62	100.76
KII-16	W	12.53	1.41	0.70	27.40	18.98	0.20	–	0.07	0.01	0.03	–	39.55	100.09
KII-19	W	16.41	0.92	0.34	23.34	19.73	0.11	0.09	0.05	0.01	–	0.01	37.58	98.57
KII-21	W	3.10	0.35	0.34	53.43	1.28	0.06	–	0.03	0.03	0.03	–	42.78	100.14
KII-22	C	11.00	0.58	0.27	29.85	16.26	0.07	–	0.03	0.01	–	–	40.94	99.00
KII-24	C	7.31	0.37	0.11	28.41	19.89	0.03	–	0.02	–	–	0.01	43.24	99.39
KII-25	W	12.37	0.71	0.30	24.86	20.46	0.09	–	0.04	0.01	–	0.01	39.83	98.67
KII-29	W	19.90	2.63	1.08	21.91	17.98	0.45	–	0.13	0.02	–	0.01	34.82	98.92
KII-31	C	16.22	1.66	0.65	24.59	18.30	0.27	0.09	0.08	0.02	–	0.01	37.23	99.11
KII-33	C	3.77	1.11	0.46	51.06	1.14	0.08	–	0.05	0.01	–	0.01	41.53	99.22
Max		45.90	2.63	1.08	53.43	20.46	0.45	0.09	0.27	0.03	0.03	0.01	44.02	101.31
Min		3.10	0.31	0.11	21.91	1.14	0.03	0.06	0.02	–	–	0.01	24.62	98.57
Mean		14.05	0.99	0.45	30.34	15.15	0.14	0.08	0.06	0.01	0.02	0.01	38.50	99.62
SS		10.89	0.67	0.24	8.81	6.73	0.11	0.01	0.06	0.01	0.01	–	5.68	0.97

ΣFe_2O_3: total iron; LOI: loss on ignition. Note: type of samples were given in Table 1.

content shows similar behavior in all sections. An homogeneous increase or decrease in SiO_2 content was not observed from bottom to top in all sections. The Ca and Mg oxide content was found to fluctuate similarly. A slightly negative correlation is seen between Si and Mg and Si and Ca. A clearly negative relation is observed between Ca and Mg. The SiO_2, Al_2O_3, Fe_2O_3 and K_2O content is greater in tuffitic layers than in other layers. The Ca/Mg ratio of the layers is >2 while the ratio is <1.60 where the main carbonate mineral is dolomite. The Mg/Ca ratios range from 0.53 to 0.81 where the main carbonate mineral is dolomite, whereas the ratio is <0.04 where the carbonate mineral is calcite. The ratios are between 0.2 and 0.50 where calcite and dolomite are found together in the same sample.

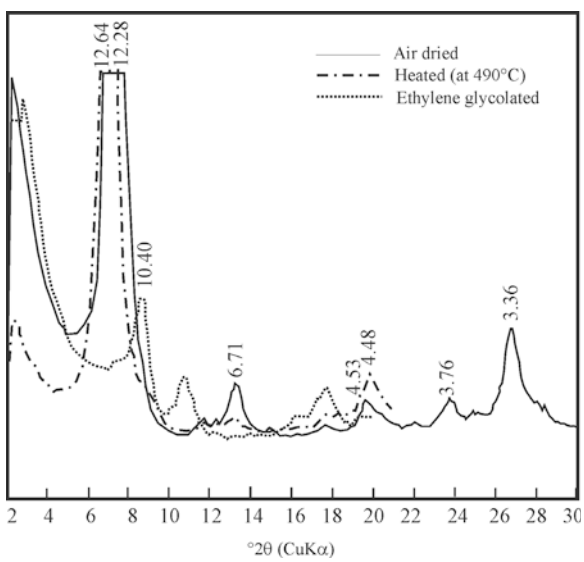

Figure 4. XRD patterns of oriented samples of the clay fraction of sample K-8_2 (cream-colored sample).

In general, the chemical compositions of the sepiolite types are similar, but the Al_2O_3 and, to some extent the CaO and K_2O content of sepiolites in organic-matter-rich layers is less than in the other layers (Table 3). The MgO content of sepiolite-rich <2 μm samples is 19.64–24.42%, and the SiO_2 content is 57.17–58.9%. The theoretical SiO_2/MgO ratio of sepiolite is 2.23, and SiO_2 is typically on the order of 55.9±1.9%, and MgO 21–25% (Jones and Galán, 1988). The SiO_2/MgO ratios of the Karapınar sepiolites range from 2.35 to 2.92, and these ratios are similar to ideal sepiolite (Weaver, 1989), whereas the SiO_2/MgO ratios are greater than the theoretical ratio of sepiolite. Furthermore, the SiO_2 content is greater than theoretical sepiolite while the MgO content is less. The differences in chemical composition reflect the mineralogy of the sediments. Using the Brauner-Preisinger model (Bailey, 1980) for ideal sepiolite, structural formulae were calculated (Table 3). The data show a relatively small substitution of tetrahedral Al for Si (0.08–0.47). Mg is the dominant cation in the octahedral site, accompanied by minor amounts of Al, Fe, Ti and rarely Cr. Octahedral cation occupancy is low and thus the extra positive charges created by Al substitution for Mg compensate only partially for the negative tetrahedral and octahedral charges. Interlayer cations are generally Ca, in some cases K, and rarely Na. The sepiolites show minor compositional differences from one section to another. The sepiolites from sections K and KI show similar

https://doi.org/10.1346/CCMN.2004.0520410 Published online by Cambridge University Press

Table 3. Major element composition (%) of clay fractions and structural formulae of sepiolites.

Oxide	K-4 (C)	K-82 (C)	K-23 (W)	KI-13 (C)	KI-19 (C)	KI-33 (W)	KII-4 (B)	KII-9 (B)	KII-19 (W)
SiO_2	57.17	58.33	57.27	58.16	58.10	57.12	59.36	59.35	58.99
Al_2O_3	2.83	4.14	5.68	3.25	2.96	3.06	1.80	1.13	2.58
ΣFe_2O_3	1.34	2.15	2.81	0.76	0.82	0.68	0.95	0.87	0.61
MnO	0.01	0.01	0.02	0.01	0.01	0.01	0.01	0.01	0.01
MgO	24.25	20.80	19.64	24.13	24.29	24.42	24.11	24.22	24.32
CaO	0.13	0.21	0.88	1.08	1.22	0.98	0.13	0.12	0.68
K_2O	0.25	0.57	0.70	0.34	0.31	0.39	0.25	0.16	0.11
Na_2O	0.03	–	–	0.06	0.08	–	0.03	–	–
TiO_2	0.16	0.23	0.32	–	–	–	0.10	0.05	0.04
P_2O_5	0.03	–	0.01	0.05	0.05	0.05	–	–	0.02
LOI	13.11	14.78	12.85	11.84	12.01	13.16	13.19	15.60	12.80
Total	99.31	101.22	100.18	99.68	99.85	99.87	99.93	101.51	100.16
Tetrahedral									
Si	11.60	11.79	11.53	11.61	11.61	11.57	11.92	12.00	11.77
Al	0.40	0.21	0.47	0.39	0.39	0.43	0.08	–	0.23
T.C.	0.40	0.21	0.47	0.39	0.39	0.43	0.08	–	0.23
Octahedral									
Al	0.27	0.77	0.88	0.37	0.33	0.30	0.35	0.27	0.38
Ti	0.02	0.04	0.05	–	–	–	0.01	0.01	0.01
Fe	0.20	0.32	0.42	0.12	0.12	0.10	0.14	0.13	0.09
Mg	7.34	6.27	5.89	7.17	7.24	7.36	7.22	7.32	7.23
T.O.C.	+0.20	0.03	0.12	0.19	0.47	0.08	0.05	0.12	0.09
O.C.	7.83	7.40	7.24	7.66	7.66	7.76	7.71	7.73	7.71
Interlayer									
Ca	0.03	0.05	0.19	0.23	0.26	0.21	0.02	0.03	0.14
Na	0.01	–	–	0.02	0.02	–	0.01	–	–
K	0.06	0.15	0.18	0.09	0.07	0.10	0.08	0.05	0.02
I.L.C.	0.13	0.25	0.56	0.57	0.61	0.52	0.13	0.11	0.30
T.L.C.	0.20	0.24	0.56	0.58	0.62	0.51	0.13	0.12	0.32

ΣFe_2O_3: total iron; LOI: loss on ignition; T.C.: tetrahedral charge; O.C.: octahedral charge; T.O.C.: total octahedral cation; I.L.C.: interlayer charge; T.L.C.: total layer charge., B: brown, C: cream, W: white sepiolite

tetrahedral substitutions and total layer charges, whereas sepiolite in section KII has little tetrahedral substitution and smaller total layer charge. The chemical composition of the Karapınar sepiolite differs significantly from the Eskişehir sepiolite (Table 3) (Ece and Çoban, 1994). All major-element oxides are greater than the Eskişehir sepiolite, except MgO and SiO_2 (Çoban, 2001). The SiO_2 and LOI values are larger or smaller in some samples, and MgO is smaller. The layer charge of the Karapınar sepiolites is also dissimilar to the Eskişehir and Yunak sepiolites.

The morphological properties of these samples were examined via SEM-EDS studies (Figures 5–7). The SEM studies were performed on whole-rock samples and the studies reveal that:

(1) The sepiolites are generally the same in shape and fiber size in most of the samples; the length of sepiolite filaments is ~5–10 μm, and the width and thickness of those <1 μm. The more abundant morphologies correspond to planar aggregates (often with filamentous borders), and filamentous-fibrous aggregates of bundle-like aspect (Figure 5). Some of the sepiolite fibers grew from anhedral dolomitic material or as coatings on dolomitic material. This type of sepiolite-fiber occurrence (from the anhedral dolomitic material) can be seen in Figure 5e. In the EDS analysis, the dolomitic material was found to contain high Ca and Mg and low Si, whereas the sepiolitic material contains high Si and Mg and low Ca (Figure 5f,g,h).

(2) Fossil-rich layers generally contain gastropod fossils and sepiolite. In particular, brown sepiolitic material contains gastropod fossils (Figure 6a,b). In EDS analyses, the chemical constituents of the gastropod inner and outer casts were found to be mainly Ca and partly Si and Mg, whereas the composition of the filling materials of the fossil casts is similar in composition to sepiolite (Figure 6c,d). However, the Ca content of the inner cast is greater than that of the outer cast.

(3) Sepiolite fibers grew from carbonaceous material in sample KII-9, and from idiomorphic-subidiomorphic dolomite rhombs (Figure 7a,b). The crystal size of dolomite is generally <2 μm. Some small dolomite rhombs grew on anhedral dolomitic material.

According to the d_{104} values of calcite, the $MgCO_3$ content of the calcite is 0–5% mole, indicating that it is low-magnesian calcite (LMC) (Goldsmith *et al.*, 1961); the results of chemical analyses corroborate this finding. The CaO/MgO molecular ratios of the dolomites range

https://doi.org/10.1346/CCMN.2004.0520410 Published online by Cambridge University Press

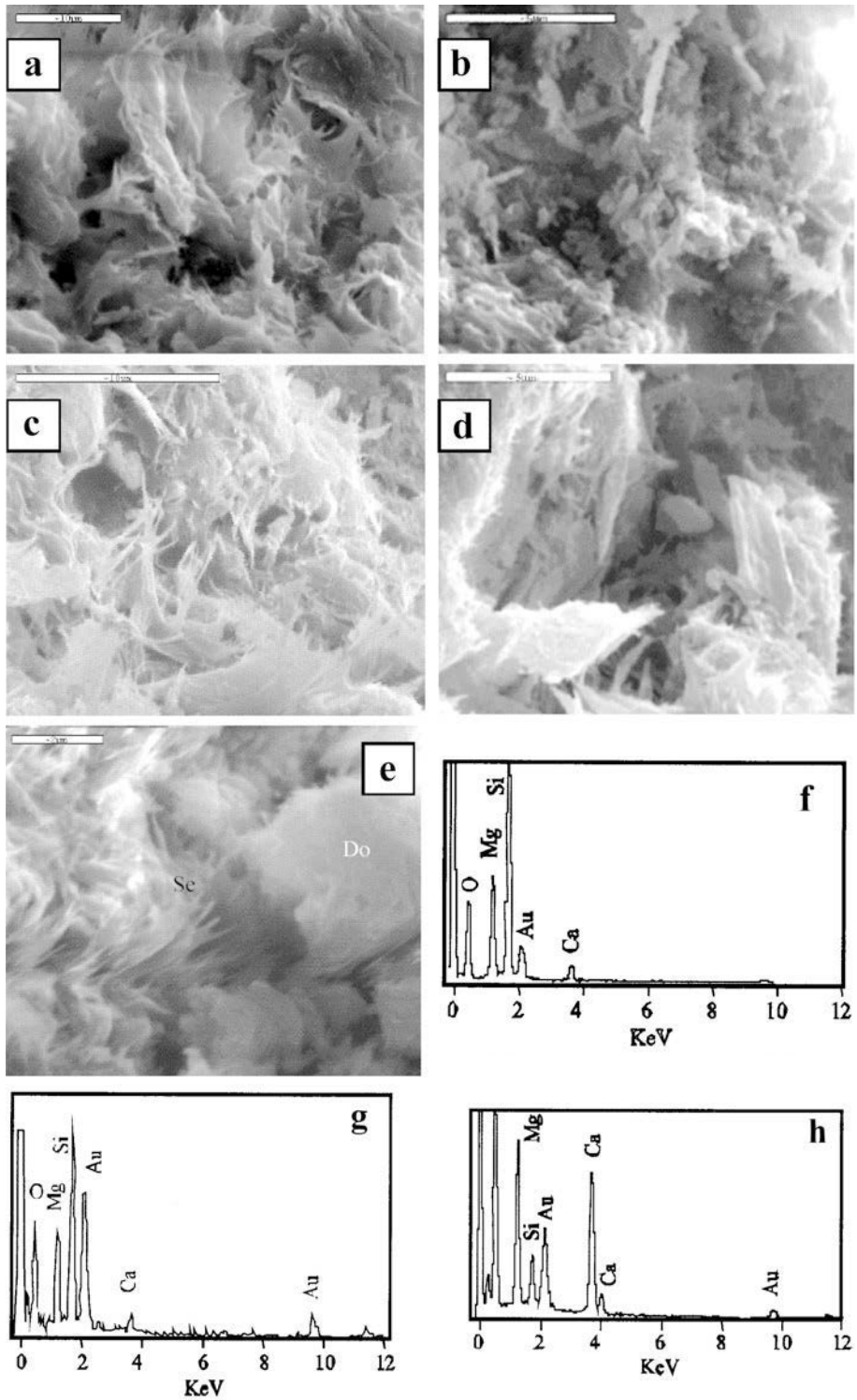

Figure 5. SEM images of sepiolite fiber masses connected to each other by bridges of fiber bundles (a–e); microcrystalline dolomite rhombs between sepiolite fibers (b); semi-quantitative analyses of sepiolite fibers (f, g) and dolomite (h).

from 1.15 to 1.35. The dolomites are rich in the Ca^{2+} ion, and are high-calcian dolomite. The Mg/Ca ratios of the dolomite-rich samples are ~0.48–0.90 in the dolomite. Calcium substitution in the dolomite was found to be ~58% $CaCO_3$ in dolomite-rich or nearly pure dolomitic samples (Table 2, sample number KI-2).

There is a gradational transition between the limestones and claystones. Broken or preserved and generally

https://doi.org/10.1346/CCMN.2004.0520410 Published online by Cambridge University Press

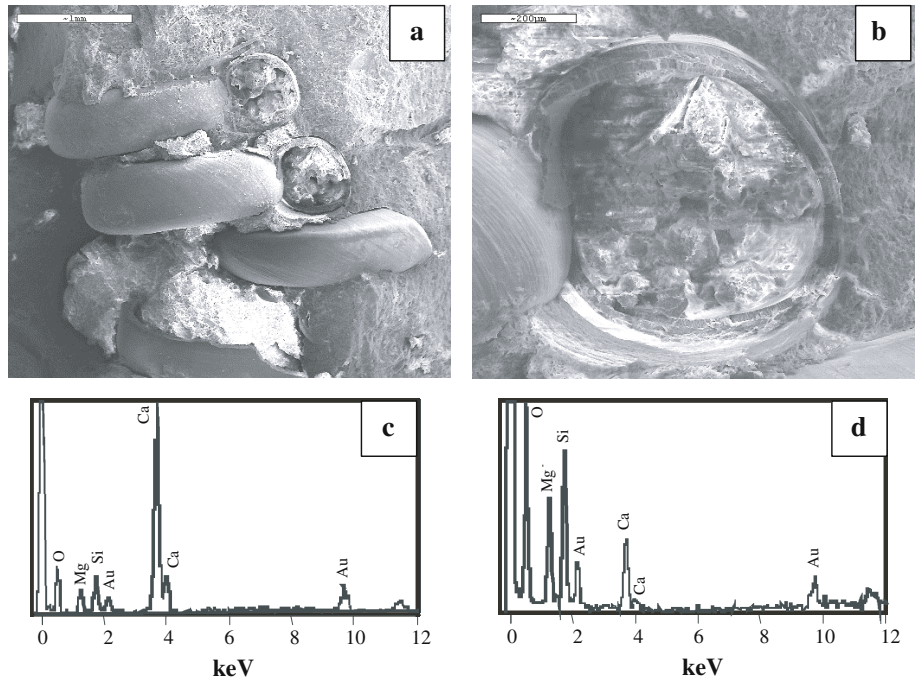

Figure 6. SEM images of gastropods (a and b), and EDS analysis of the fossil cast (c) and filling material, resembling the chemical composition of sepiolite (d).

recrystallized or dolomitized ostracods and gastropods shells are more abundant in the claystones than in the limestone layers, and some have isopachous micritic envelopes, probably developed by biological activity of endolithic organisms. The ostracods were deposited in a fresh-water environment and they are abundant mainly in claystone, marl and to some extent in the limestone and sandy limestone layers, while they are rare or absent in siliceous nodule-rich layers. Some clay-rich layers which are rich in sepiolite contain nearly 20−30% fossil material.

DISCUSSION

The Karapınar basin is located in the closed Tuz Gölü basin. In this type of closed lake, evaporation leads to elemental supersaturation in lake water and consequent mineral precipitation. These precipitated minerals strongly reflect the lake-water chemistry at the time of their deposition. The Karapınar basin lake sediments consist mainly of dolomite, calcite and sepiolite, with lesser quartz, palygorskite and feldspar, and scarce mica and opal-CT.

Sepiolite appears to have formed partially by displacement of dolomites and/or by direct precipitation from solution, as suggested by SEM photomicrographs and EDS analyses (Figures 5e, 6a,b). The chemical composition of gastropod fill material is similar to that of sepiolite, and the chemical composition of the fossil casts is mainly Ca and, in some cases, Si and Mg. The presence of gastropods and ostracods indicates a fresh-

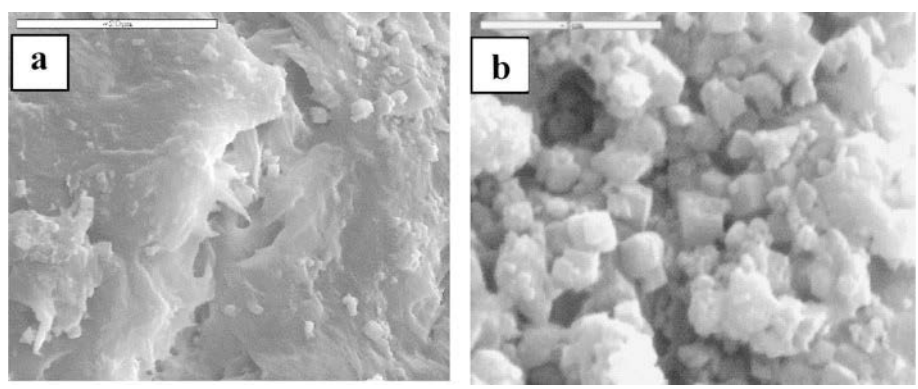

Figure 7. SEM images of sepiolite growth from whole-rock material (sample KII-9), microcrystalline dolomite rhombs (a) and euhedral-subhedral dolomite rhombs (b).

https://doi.org/10.1346/CCMN.2004.0520410 Published online by Cambridge University Press

water environment. It is thought that after the death of the organism, sepiolitic material precipitated during seasonal evaporation, resulting in fluctuations of salinity between saline and fresh-water conditions. Oscillations of lake level and variations in water chemistry usually result in the deposition of a wide variety of carbonate minerals, with calcite precipitating when the water is fresh, and Mg-calcite, protodolomite, dolomite and sepiolite precipitating when the water is brackish to saline (Hsü and Kelts, 1978). Occurrences of fibrous clay minerals as coatings on carbonate grains and as pore fillings were observed in the study area and were also reported by Hassouba and Shaw (1980), Estéoule-Choux (1984), Yalçın and Bozkaya, (1995) and many others; they were interpreted to be of authigenic rather than detrital origin. The SEM observations and XRD determinations of sepiolite samples and sepiolite + palygorskite samples without smectite or other clay mineral, suggest that the sepiolites may have formed by two mechanisms: (1) mainly from dolomite and, more rarely, from palygorskite; and (2) as a direct precipitate from solution.

Silicic acid forms as a result of chemical weathering of volcanic rocks containing silicate minerals such as feldspars, micas and pyroxenes rather than by solution of crystalline or amorphous SiO_2. Silicon dioxide reacts with water to form silicic acid, such that at equilibrium (Faure, 1998):

$$SiO_2 \text{ (amorph)} + 2H_2O \rightarrow H_4SiO_4$$

Reactions of pore-waters rich in silicic acid with dolomite suggest the following:

$$8\underset{\text{dolomite}}{CaMg(CO_3)_2} + 12H_4SiO_4 \rightarrow \underset{\text{sepiolite}}{Mg_8Si_{12}O_{30}(OH)_4(OH_2)_4.8H_2O} + 8Ca^{2+} + 16HCO_3^- + 2H_2O$$

and

$$Mg_2(Al,Fe^{3+})_2Si_8O_{20}(OH)_2(OH_2)_4.4H_2O + 6Mg^{2+} + 4H_4SiO_4 + 6(OH^-) \rightarrow \underset{\text{palygorskite}}{} \underset{\text{sepiolite}}{Mg_8Si_{12}O_{30}(OH)_4(OH_2)_4.8H_2O} + 6H_2O + (Al, Fe^{3+})_2$$

Sepiolite occurs as a major phase in all layers, and is closely related to the formation of carbonate minerals. Experimental studies establish the necessity of an alkaline solution (pH 8) and silica concentrations in aqueous solution controlled by the presence of amorphous silica (20–150 ppm) in order to precipitate sepiolite (Wollast *et al*., 1968). According to Jones and Galán (1988), both sepiolite and palygorskite commonly form by a dissolution-precipitation mechanism which incorporates components of pre-existing detrital material. The absence of detrital sheet minerals supports the hypothesis that sepiolite forms by chemical precipitation and not by transformation of precursor minerals, such as palygorskite (Bachman and Machette, 1977). Measurement of Mg^{2+}, H^+ and SiO_2 concentrations in solution after precipitation of sepiolite demonstrates the relatively constant pH and Mg^{2+}-SiO_2 concentrations of the supernatant liquid. The result of these experiments is to establish that the precipitation of sepiolite from solution can occur at pH.8.2, with 56 mmoles Mg^{2+} and 0.4 mmoles SiO_2 concentration (Velde, 1985). Silica nodules and silica-rich layers in the carbonate rocks indicate that the environment was saturated with silicic acid and favored the formation of sepiolite. Kastner (1986) showed that Mg^{2+} can be removed from suspensions containing amorphous silica at low temperatures by adsorption and precipitation of a Mg-hydrosilicate which resembles sepiolite. Silicon, Mg, Al and Fe may have been derived from basic volcanites and/or volcanic ash as a result of hydrolysis of mafic minerals and plagioclase in the lacustrine environment. The MgO content of basic volcanites is between 6.30 and 8.25 in the central Anatolian and Karapınar regions (Olanca, 1999; Şen *et al*., 2004). Calcium may have been derived from dissolution of carbonate rocks in the surrounding area and/or from dissolution of plagioclase (anorthite) in the basic volcanites and ash. Mg^{2+} may have been supplied by circulation of groundwaters with high Mg content. Precipitation of sepiolite is only likely to occur in the sediment column where temperatures are >~10ºC and is most likely to form from carbonate-containing siliceous sediments where $CaCO_3$ dissolution helped to maintain pH values $\geqslant$8.0. In other words, a Mg-clay (especially sepiolite) + dolomite assemblage may develop when the Mg/Ca ratio is high; an assemblage of Mg-clay (palygorskite, smectite) and/or calcite develops if this ratio is lower (Harder, 1972). Dissolution of basic volcanites may have produced the Mg/Ca ratios and high salinities in pore-water necessary for the formation of dolomite and sepiolite. Coexisting dolomite and sepiolite indicate that the Mg content of the lake was sufficient for this sort of occurrence of dolomite and subsequent precipitation of sepiolite. Dolomite-sepiolite associations were observed locally in both vertical and lateral distributions of clay-carbonate minerals in the Karapınar region. Occurrences of silica nodules and silica lenses in the carbonate rocks indicate that the environment was saturated in silicic acid and that silica may have been derived from the dissolution of basic volcanic rocks; this is only likely to occur in the sediment column where temperatures are >~10ºC (Velde, 1985).

The absence of any detrital clay minerals, such as smectite or illite, indicates that no significant overland run-off occurred. Minor amounts of quartz and feldspar may have been the result of some short-lived eolian input and/or been derived from contemporaneous volcanic ash from nearby volcanic activity.

https://doi.org/10.1346/CCMN.2004.0520410 Published online by Cambridge University Press

Based upon the results of mineralogical and chemical analyses, the dolomites are protodolomite and the calcites are low-Mg calcite. Müller *et al*. (1972) indicated that the offshore Holocene sediments of the Tuz Gölü basin are composed of dolomite associated with huntite, magnesite and various evaporitic sulfates, and that the dolomite is poorly ordered and Ca-rich. They also maintained that large amounts of high-Mg calcite precipitate from the lake water on a seasonal basis, and that dolomite is interpreted as a product of this high-Mg calcite. Last (1990) suggested that primary calcite or aragonite is deposited during periods of relatively high water level. These primary carbonates were quickly altered to dolomite by the high Mg/Ca ratio of the basin. In the study area, sepiolite is associated with dolomite, dolomite and calcite and, more rarely, calcite. However, gypsum occurrences were not observed, its absence indicating that open, hypersaline-evaporatic basin conditions were not present. The occurrence of organic matter-rich sepiolite beds indicates the presence of water stratification with bottom-water anoxia in the deepest part of the lake.

CONCLUSIONS

The Karapınar basin was a small part of the closed Konya paleolake. Some parts of the paleolake varied from saline to brackish to fresh-water, and some of them became oversaturated due to the high input of alkaline, continental groundwaters. In these closed lakes, evaporation leads to elemental supersaturation in water, and to consequent mineral precipitation. These precipitated minerals strongly reflect the lake-water chemistry at the time of their deposition. Fluctuations in lake-water level and variations in water chemistry usually result in the deposition of a wide variety of carbonate minerals, with calcite precipitating when the water is fresh, while magnesian calcite, protodolomite and dolomite are deposited when the water is brackish to saline (Hsü and Kelts, 1978). Thus, calcite and low-Mg calcite precipitation occurred in periods of high water with low rates of evaporation, whereas high-Mg calcite, protodolomite and dolomite precipitation occurred during periods of low-water level and high evaporation in the Karapınar basin (Landmann *et al*., 1996). The presence of sepiolite is closely related to the formation of carbonate minerals. Sepiolite formed in equilibrium with silica under very alkaline conditions (pH 8.2) with high Mg^{2+} concentration. Sepiolite was precipitated where Mg and Si are available and where detrital components were almost non-existent. Palygorskite generally occurs where Al^{3+} is high in solution. In the Karapınar basin, Al content was low in all samples except tuffitic layers, so minor palygorskite precipitation occurred in a few layers. The chemical compositions of the sepiolites are generally similar to ideal sepiolite and other Turkish sepiolites. The relatively high SiO_2 content compared to theoretical sepiolite indicates that Si concentration was high during the precipitation of sepiolite. The sepiolite-smectite relation was established for other Turkish sepiolites insofar as smectite was not observed in the Karapınar basin. Subsurface waters, concentrated with respect to certain anions and cations, descended along fracture systems in the basin under highly evaporative conditions, and may have caused precipitation of sepiolite, and possibly palygorskite and some carbonate minerals, depending on environmental conditions during waning detrital and volcanic activity. Magnesium was derived primarily from the volcanites and partially from the ophiolites. Silica and Mg may have been sourced from high-Mg volcanites.

ACKNOWLEDGMENTS

The authors gratefully acknowledge Dr Warren Huff's contributions and constructive reviews of the manuscript. We also thank Dr D.C. Bain for his helpful suggestions.

REFERENCES

Albee, A.L. and Ray, L. (1970) Correction methods for electron microprobe microanalysis of silicates, carbonates, phosphates, and sulfates. *Analytical Chemistry*, **42**, 1408–1414.

Aydar, E. (1989) *Les lavas quaternaires de Cappadoce (Turquie): Volcanologie et Petrologie*. D.E.A. Géosciences. Université Blaise Pascal, Clermont-Ferrand, France, 48 pp.

Bachman, G.O. and Machette, M.N. (1977) Calcic soils and calcretes in the southwestern United States. *US Geological Survey, Open-File Report* 77-794, 163 pp.

Bailey, S.W. (1980) Structures of layer silicates. Pp. 1–123 in: *Crystal Structures of Clay Minerals and their X-ray Identification* (G.W. Brindley, and G. Brown, editors). Monograph **5**, Mineralogical Society, London.

Bain, D.C. and Smith, B.F.L. (1987) Chemical analysis. Pp. 248–274 in: *A Handbook of Determinative Methods in Clay Mineralogy* (M.J. Wilson, editor). Chapman & Hall, London.

Brown, G.C., Hughes, D.J. and Esson, J. (1973) New XRF data retrieval techniques and their application to U.S.G.S. standard rocks. *Chemical Geology*, **11**, 223–229.

Collinson, J.D. (1978) Lakes. Pp. 61–79 in: *Sedimentary Environments and Facies* (H.G. Reading, editor). Blackwell, Oxford, UK.

Çoban, F. (2001) Ahiler (Sivrihisar-Eskişehir) sepiyolitinin jeokimyasal özellikleri. *Yerbilimleri*, **39**, 13–30.

Ece, Ö.I. (1998) Diagenetic transformation of magnesite pebbles and cobbles to sepiolite (meerschaum) in the Miocene Eskişehir lacustrine basin, Turkey. *Clays and Clay Minerals*, **46**, 436–445.

Ece, Ö.I. and Çoban, F. (1994) Geology, occurrence and genesis of Eskişehir sepiolites, Turkey. *Clays and Clay Minerals*, **42**, 81–92.

Ercan, T., Tokel, S., Can, B., Fişekçi, A., Fujitani, T., Notsu, K., Selvi, Y., Ölmez, M., Matsuda, J.I., Ui, T., Yıldırım, T. and Agırbaşlı, A. (1992) Hasandag-Karacadag (Orta Anadolu) dolayındaki Senozoyik yaşlı volkanizmanin kökeni ve evrimi. *Jeomorfoloji Dergisi*, **18**, 39–54.

Estéoule-Choux, J. (1984) Palygorskite in the Tertiary deposits of the Armorican Massif. Pp. 75–85 in: *Palygorskite-Sepiolite, Occurrences, Genesis and Uses* (A. Singer and E. Galán, editors). Developments in Sedimentology, **37**.

Elsevier, Amsterdam.
Faure, G. (1998) *Principles and Applications of Geochemistry*, 2nd edition. Prentice-Hall, London, 600 pp.
Flanagan, F.J. (1976) Description and analyses of eight new USGS rock standards: In twenty eight papers presenting analytical data on standards (F.J. Flanagan, editor). *USGS Professional Paper*, **840**, 171–172.
Galán, E. and Ferrero, A. (1982) Palygorskite-sepiolite clays of Lebrija, southern Spain. *Clays and Clay Minerals*, **30**, 191–199.
Gibbs, R.J. (1965) Error due to segregation in quantitative clay mineral X-ray diffraction mounting techniques. *American Mineralogist*, **50**, 741–751.
Gibbs, R.J. (1968) Clay mineral mounting techniques for X-ray diffraction analyses. A discussion. *Journal of Sedimentary Petrology*, **38**, 242–244.
Govindaraju, K. (1989) Compilation of working values and sample description for 272 geostandards: *Geostandards Newsletter*, **13**, 1–113.
Goldsmith, J.R., Graff, D.L. and Heard, H.C. (1961) Lattice constants of the calcium-magnesium carbonates. *American Mineralogist*, **46**, 453–457.
Gündoğdu, M.N. (1982) *Neojen yaşlı Bigadiç sedimanter baseninin jeolojik, mineralojik ve jeokimyasal incelenmesi*. PhD thesis, Hacettepe Universitesi, Turkey, 386 pp.
Harder, H. (1972) The role of magnesium in the formation of smectite minerals. *Chemical Geology*, **10**, 31–39.
Hassouba, H. and Shaw, H.F. (1980) The occurrence of palygorskite in Quaternary sediments of the coastal plain of North-west Egypt. *Clay Minerals*, **15**, 77–83.
Hewett, D.F. (1956) Geology and mineral resources of the Wanpal Quadrangle, California and Nevada. *US Geological Survey Professional Paper* **275**, 143–144.
Hsü, K.J. and Kelts, K. (1978) Late Neocene chemical sedimentation in Black Sea. Pp. 129–145 in: *Modern and Ancient Lake Sediments* (A. Matter and M.E. Tucker, editors). Special Publication **2**, International Association of Sedimentology. Blackwell, Oxford, UK.
Jackson, M.L. (1975) *Soil Chemical Analysis – Advanced Course*, 2nd edition. Published by the author. Madison, Wisconsin, 985 pp.
JCPDS (1993) *Mineral Powder Diffraction File Databook:* Joint Committee on Powder Diffraction Standards, Swarthmore, Pennsylvania, 781 pp.
Jones, B.F. and Galán, E. (1988) Sepiolite and palygorskite. Pp. 631–674 in: *Hydrous Phyllosilicates (exclusive of Micas)* (S.W. Bailey, editor). Reviews in Mineralogy **19**, Mineralogical Society of America, Washington, D.C.
Kadir, S., Baş, H. and Karakaş, Z. (2002) Origin of sepiolite and loughlinite in a Neocene sedimentary lacustrine environment, Mihalıççık-Eskişehir, Turkey. *The Canadian Mineralogist*, **40**, 1091–1102.
Karakaya, N., Karakaya, M.Ç., Temel, A. and Küpeli, Ş. (2001) Neojen yaşlı Karapınar formasyonunun (Konya Doğusu) mineralojisi ve jeokimyası. *Proceedings of the 10th National Clay Conference*, pp. 213–220.
Kastner, M. (1986) New insight into origin of dolomite. *12th International Sedimentology Congress, Canberra*, pp. 158–159.
Landmann, G., Reimer, A. and Kempe, S. (1996) Climatically induced lake level changes at Lake Van, Turkey, during the Pleistocene/Holocene transition. *Global Biogeochemical Cycles*, **10**, 797–808.
Last, W.M. (1990) Lacustrine dolomite: an overview of modern, Holocene, and Pleistocene occurrences. *Earth-Science Reviews*, **27**, 221–263.
Mayayo, M.J., Torres-Ruíz, J., González-López, J.M., López-Galindo, A. and Bauluz, B. (1998) Mineralogical and chemical characterization of the sepiolite/Mg-smectite deposit at Mara (Calatayud basin, Spain). *European Journal of Mineralogy*, **10**, 367–383.
Millot, G. (1970) *Geology of Clays*. Chapman & Hall, London, 429 pp.
Müller, G., Irion, G. and Förstner, U. (1972) Formation and diagenesis of inorganic Ca-Mg carbonates in the lacustrine environment. *Naturwissenschaften*, **59**, 158–164.
Olanca, K. (1999) Karapınar-Konya yöresi Kuvaterner volkanizmasi: Jeokimyasal yorum. *Hacettepe Üniversitesi Yerbilimleri Dergisi*, **21**, 115–124.
Post, J.L. (1978) Sepiolite deposits of the Las Vegas, Nevada area. *Clays and Clay Minerals*, **26**, 58–64.
Şen, P.A., Temel, A. and Gourgaud, A. (2004) Petrogenetic modeling of Quaternary post-collision volcanism: a case study of Central and Eastern Anatolia. *Geological Magazine*, **141**, 81–98.
Shadfan, H., Mashhady, A.S., Dixon, J.B. and Hassen, A.A. (1985) Palygorskite from Tertiary formations of Eastern Saudi Arabia. *Clays and Clay Minerals*, **33**, 451–457.
Temel, A., Gündogdu, M.N and Gourgaud, A. (1998) Petrological and geochemical characteristics of Cenozoic high-K calc-alkaline volcanism in Konya, central Anatolia, Turkey. *Journal of Volcanology and Geothermal Research*, **85**, 327–354.
Velde, B. (1985) *Clay Minerals, a Physico-chemical Explanation of their Occurrence*. Developments in Sedimentology, **40**, Elsevier, Amsterdam, 427 pp.
Yalçın, H. and Bozkaya, Ö. (1995) Sepiolite-palygorskite from the Hekimhan region, Turkey. *Clays and Clay Minerals*, **43**, 705–717.
Yeniyol, M. (1986) Vein-like sepiolite occurrence as a replacement of magnesite in Konya, Turkey. *Clays and Clay Minerals*, **34**, 353–356.
Yeniyol, M. (1995) Meerschaum sepiolite and palygorskite occurrence in Central Anatolia, Turkey. *Proceedings of the 10th International Clay Conference, Adelaide*, pp. 378–382.
Weaver, C.E. (1989) *Clays, Muds and Shales*. Developments in Sedimentology, **44**. Elsevier, Amsterdam, 819 pp.
Wollast, R., Mackenzie, F.T. and Bricker, O.P. (1968) Experimental precipitation and genesis of sepiolite at earth-surface conditions. *American Mineralogist*, **53**, 1645–1662.

(*Received 6 August 2003; revised 30 March 2004; Ms. 825: A.E. Warren D. Huff*)